Octahedral Metal Carbonyls. 77.[1] Kinetics of Chelate Ring Closure via Olefin-Tungsten Bond Formation in Chlorobenzene Solvates of Tungsten Carbonyl Intermediates

Shulin Zhang, I-Hsiung Wang, Paul H. Wermer, Charles B. Dobson, and Gerard R. Dobson*

Department of Chemistry and Center for Organometallic Research, University of North Texas, Denton, Texas 76203-5068

Received June 27, 1991

The kinetics and mechanism of chelate ring closure in a series of *cis*-(CB)(η^1-P-ol)W(CO)$_4$ transients produced via pulsed laser flash photolysis from *cis*-(pip)(η^1-P-ol)W(CO)$_4$ complexes in CB solution (CB = chlorobenzene; pip = piperidine; P-ol = $Ph_2P(CH_2)_nCH{=}CH_2$, n = 1-4) have been investigated. In the presence of pip, competitive solvent displacement reactions via chelate ring closure and pip attack at the transients are observed. Studies of chelate ring closure in CB-hep solvent mixtures (hep = n-heptane) and of solvent displacement from photogenerated *cis*-(CB)(Ph_2MeP)W(CO)$_4$ by pip and 1-hexene were also carried out. These investigations indicate that for reactions of *cis*-(CB)(Ph_2MeP)W(CO)$_4$ with 1-hexene a single CB-displacement reaction pathway is accessible but that chelate ring closure in *cis*-(CB)(η^1-ol-P)W(CO)$_4$ complexes takes place via two competitive CB displacement pathways. The rate data and activation parameters indicate that all these pathways involve the intermediacy of species in which Ph_2MeP or P-ol hydrogens (ring or chain) are agostically bonded to the metal.

Introduction

Recently, it has been found that solvent (solv) displacement from (solv)M(CO)$_5$ complexes by Lewis bases (L) (e.g., Scheme I) can take place via competitive dissociative and interchange pathways.[2-4] A potentially useful way to study the interchange pathway is to probe desolvation which accompanies chelate ring closure, for which a high "local concentration" of the free end of the bidentate ligand is expected.[5] Recently, the series of *cis*-(pip)(η^1-ol-P)W(CO)$_4$ complexes (P-ol = $Ph_2P(CH_2)_nCH{=}CH_2$; n = 1-4; pip = piperidine), in which initial coordination of P-ol to the metal takes through P, were prepared.[6] This series is well-suited to desolvation studies; the accessibility of an interchange mechanism is expected to change in predictable ways based upon entropy effects which accompany the formation of chelate rings of various sizes.[7] It has been shown that flash photolysis of a member of that series, *cis*-(pip)(η^1-$Ph_2P(CH_2)_4CH{=}CH_2$)W(CO)$_4$, in chlorobenzene solution (CB) affords chelate ring closure via the intermediacy of a solvated species (Scheme II).[8] While olefin bond migration has been observed to accompany chelate ring closure in several group VIB metal carbonyl derivatives (M = Cr, Mo, W) containing P-ol ligands,[9] it has been found *not* to take place in this series of photolysis precursors.[6,8] Herein are reported mechanistic studies of these complexes after pulsed laser flash photolysis, together with comparative studies of the reaction of *cis*-(pip)(Ph_2MeP)W(CO)$_4$ with the monodentate ligand, 1-hexene (Scheme III).

Scheme I

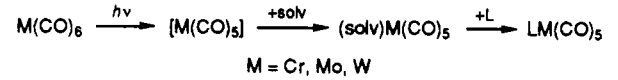

Scheme II

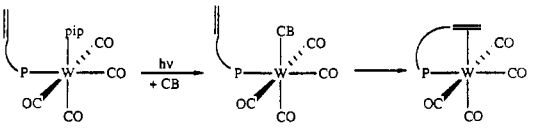

Scheme III

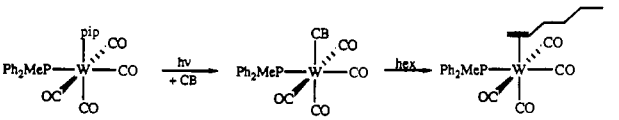

Experimental Section

Reagents. Chlorobenzene (CB, Aldrich) was purified by distillation from phosphorus pentoxide under nitrogen; n-heptane (hep, Aldrich) and methyldiphenylphosphine (Aldrich) were similarly distilled from sodium. Piperidine (pip, Lancaster Synthesis, Ltd.) was distilled from KOH, while 1-hexene (hex, Aldrich) was distilled from anhydrous $MgSO_4$. W(CO)$_6$ (Pressure Chemical Co.) was used as obtained.

The *cis*-(pip)(η^1-ol-P)W(CO)$_4$ complexes (P-ol: $Ph_2PCH_2CH{=}CH_2$, 2-propenyldiphenylphosphine, prdpp; $Ph_2PCH_2CH_2CH{=}CH_2$, 3-butenyldiphenylphosphine, bdpp; $Ph_2PCH_2CH_2CH_2CH{=}CH_2$, 4-pentenyldiphenylphosphine, pdpp; $Ph_2PCH_2CH_2CH_2CH_2CH{=}CH_2$, 5-hexenyldiphenylphosphine, hdpp) were those synthesized as described in an earlier study.[6] The synthesis of *cis*-(pip)(Ph_2MeP)W(CO)$_4$ from *cis*-(pip)$_2$W(CO)$_4$ employed the methods of Darensbourg and Kump.[10] Anal. Calcd (Midwest Microlab, Indianapolis, IN) for $C_{22}H_{24}NPO_4W$: C, 45.46; H, 4.16. Found: C, 45.55; H, 4.14. Carbonyl stretching absorptions (Nicolet 20 SXB FTIR spectrometer, cyclohexane solution): 2011 (s), 1903 (s), 1884 (vs), 1865 (s) cm^{-1}. This complex was further characterized by ^{13}C and ^1H NMR spectrometry (Varian VXR 300 FT-NMR spectrometer, $CDCl_3$ solution); these data are presented in supplementary Table I.

Reaction Products. It has been shown that upon continuous wave photolysis, *cis*-(pip)(P-ol)W(CO)$_4$ complexes undergo chelate ring closure without olefin bond migration to afford the ring-closed (η^3-P-ol)W(CO)$_4$ products.[6] Flash photolysis studies in CB of *cis*-(pip)(L)W(CO)$_4$ complexes in which ligands L are very closely related to P-ol, e.g., where L = Ph_3P and $PhMe_2P$, provided very strong evidence that *cis*-(CB)(η^1-ol-P)W(CO)$_4$ transients are formed in predominant concentration; the visible spectra for the species produced immediately after flash pho-

(1) Part 76: Asali, K. J.; Awad, H. H.; Kimbrough, J. F.; Lang, B. C.; Watts, J. M.; Dobson, G. R. *Organometallics* **1991**, *10*, 1822.
(2) Zhang, S.; Dobson, G. R. *Inorg. Chim. Acta* **1989**, *165*, L11.
(3) Zhang, S.; Dobson, G. R.; Zang, V.; Bajaj, H. C.; van Eldik, R. *Inorg. Chem.* **1990**, *29*, 3477.
(4) Zhang, S.; Dobson, G. R. *Organometallics*, in press.
(5) Schwarzenbach, G. *Helv. Chim. Acta* **1952**, *35*, 2344.
(6) Wang, I-H.; Wermer, P. H.; Dobson, C. B.; Dobson, G. R. *Inorg. Chim. Acta* **1991**, *183*, 31.
(7) Illuminati, G.; Mandolini, L. *Acc. Chem. Res.* **1981**, *14*, 95.
(8) Awad, H. H.; Dobson, G. R.; van Eldik, R. *J. Chem. Soc., Chem. Commun.* **1987**, 1839.
(9) (a) Interrante, L. V.; Bennett, M. A.; Nyholm, R. S. *Inorg. Chem.* **1966**, *5*, 2212. (b) Nyholm, R. S. *Pure Appl. Chem.* **1971**, *27*, 1078.
(10) Darensbourg, D. J.; Kump, R. L. *J. Am. Chem. Soc.* **1978**, *27*, 3308.

0020-1669/92/1331-3482$03.00/0

tolysis of *cis*-(pip)(L)W(CO)$_4$ and *cis*-(pip)(P-ol)W(CO)$_4$ complexes are essentially identical.[6,11] This evidence, together with carbonyl stretching spectra taken during the course of these reactions, and isosbestic points observed for time-resolved UV–visible spectra recorded after flash photolysis indicate that these reactions proceed cleanly according to Scheme II.

In *cis*-(CB)(L)W(CO)$_4$ intermediates, CB is coordinated to W via a lone pair on Cl and the same is likely to be true for *cis*-(CB)(η^1-P-ol)W(CO)$_4$ transients. This conclusion is based on the systematics observed for desolvation, for which, where $k_{desov,benzene} < k_{desolv,CB}$, CB is coordinated through the ring, while, where the reverse is true, CB is coordinated to M via a lone pair on Cl.[11,12]

Flash Photolysis Studies. Flash photolysis studies were carried out at the Center for Fast Kinetics Research as previously described[13] employing a Quantel YG481 Nd:YAG laser at 355 nm (11-ns fwhi) or in our laboratories, also as described previously,[14] employing a Tachisto Model 800 excimer laser (351 nm, Xe/F_2/He gas fill, 14-ns fwhi); results were reproducible by employing either system. Solutions ca. 5×10^{-3} M in the metal carbonyl complex with at least a 20-fold excess of pip or 1-hexene (hex) "trap" (if a trap was utilized) were employed to ensure pseudo-first-order rate behavior. Temperatures were maintained within ±0.05 °C through use of a 1-cm jacketted cell and external circulating bath.

Depending upon the signal-to-noise ratio obtained, the pseudo-first-order rate constants obtained from plots of ln ($A_t - A_\infty$) vs time were determined from averages of 1–10 traces. The observation wavelengths were 430 nm (data in supplementary Table II) and 470 nm (data in supplementary Tables III and IV). No significant differences were observed for individual traces obtained after the first or subsequent flashes, which indicates that flash photolysis of the substrates affords the same intermediates as does flash photolysis of the reaction products. The data, obtained as values of k_{obsd}, the pseudo-first-order rate constants (supplementary Tables II–IV), were analyzed at CFKR or in-house, by employing Asyst-based computer programs and a laboratory microcomputer. Limits of error are given in parentheses as the uncertainties of the last digit(s) of the cited values to one standard deviation.

Results

Determination of the Values of k_{obsd} for Reactions of *cis*-(CB)(η^1-ol-P)W(CO)$_4$ and *cis*-(CB)(Ph$_2$MeP)W(CO)$_4$ Complexes Produced after Flash Photolysis. Studies of desolvation in *cis*-(CB)(L)W(CO)$_4$ intermediates[11] set the conditions for study of the *cis*-(pip)(η^1-ol-P)W(CO)$_4$ complexes. Flash photolysis of the latter and of *cis*-(pip)(Ph$_2$MeP)W(CO)$_4$ in CB/pip solutions ([pip] ≤ 1 M) afforded plots of relative absorbance vs time which exhibited exponential decay, together with linear plots of ln ($A_t - A_\infty$) vs time (A_t and A_∞ are the relative absorbances at time t and infinite time, respectively), indicative of pseudo-first-order rate behavior. Typical plots, for chelate ring closure in *cis*-(CB)(η^1-hdpp)W(CO)$_4$ at 25.0 °C, ([pip] = 0) monitoring 470 nm, are shown in Figure 1. The decay of the intermediate to a baseline lower than that observed prior to photolysis is indicative of the formation of a product containing a coordinated olefin; it has been observed that the visible absorptions for species containing coordinated olefins are significantly blue-shifted from those of the photolysis precursors from which they are produced.[3] Values of k_{obsd}, the pseudo-first-order rate constants for disappearance of the photogenerated *cis*-(CB)(η^1-ol-P)W(CO)$_4$ and *cis*-(CB)(Ph$_2$MeP)W(CO)$_4$ intermediates were obtained from the slopes of the linear plots. These values are given in supplementary Tables II–IV.

Observed Rate Behavior. (a) Reactions of *cis*-(CB)(η^1-ol-P)W(CO)$_4$ and *cis*-(CB)(Ph$_2$MeP)W(CO)$_4$ in CB/pip Solutions. Plots of k_{obsd} vs [pip]/[CB] (<0.14) for decay of the five transients, *cis*-(CB)(CH$_2$=CH(CH$_2$)$_n$PPh$_2$)W(CO)$_4$ (n = 1–4) and *cis*-(CB)(Ph$_2$MeP)W(CO)$_4$ at 26.1 °C are illustrated in Figure 2. The data are encompassed within the rate law

$$k_{obsd} = k_a + k_b[pip]/[CB] \quad (1)$$

Note that finite intercepts are observed for the P-ol complexes but not for Ph$_2$MeP, suggesting that the unimolecular pathway governed by k_a involves chelate ring closure. Values of k_{obsd} for data taken over the temperature range 14.5–38.7 °C are presented in supplementary Table II, while the corresponding rate constants, k_a and k_b, are listed in Table I.

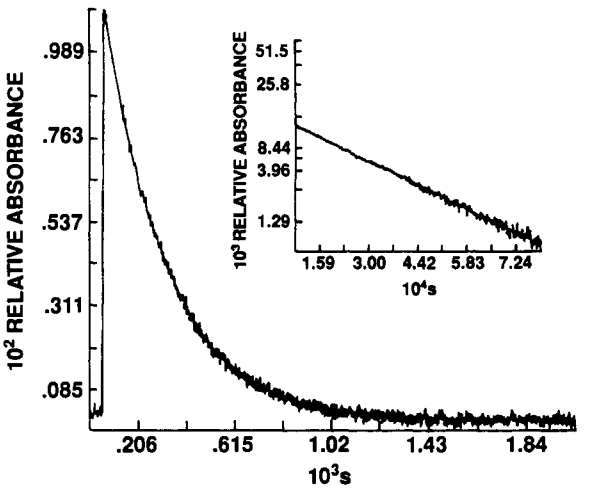

Figure 1. Plot of relative absorbance vs time, monitoring at 470 nm, for the reaction taking place after flash photolysis of *cis*-(pip)(η^1-hdpp)W(CO)$_4$ in CB solution ([pip] = 0 M) at 25.0 °C. The inset shows the corresponding plot of ln ($A_t - A_\infty$) vs time.

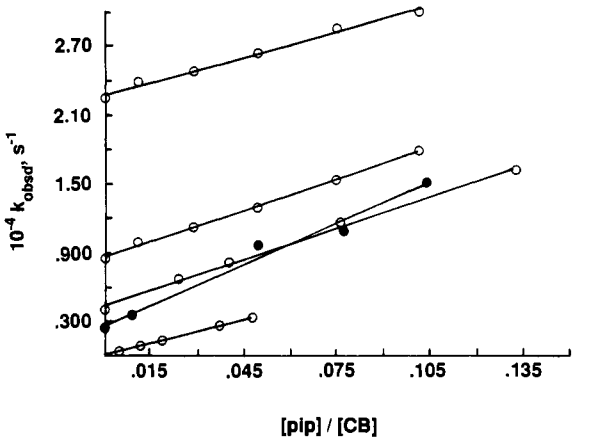

Figure 2. Plots of k_{obsd} vs [pip]/[CB] for reactions of *cis*-(CB)(η^1-P-ol)W(CO)$_4$ intermediates and *cis*-(CB)(Ph$_2$MeP)W(CO)$_4$ in CB–pip solutions at 26.1 °C. Plots, bottom to top, at y intercept: L = Ph$_2$MeP, pdpp, hdpp, bdpp, prdpp.

(b) Reaction of *cis*-(CB)(Ph$_2$MeP)W(CO)$_4$ with 1-Hexene in Chlorobenzene. The displacement of CB from photogenerated *cis*-(CB)(Ph$_2$MeP)W(CO)$_4$ by 1-hexene (hex) to afford *cis*-(hex)(Ph$_2$MeP)W(CO)$_4$ (Scheme III) offers the opportunity to compare solvent displacement reactions for systems differing principally in the presence or absence of the chelate ring. This reaction was studied over a wide range of [hex]/[CB], 0.17–2.0.[15] Plots of k_{obsd} vs [hex]/[CB] for data taken over the temperature range 5.0–25.0 °C are shown in Figure 3. These plots, curved downward and passing through the origin, are suggestive

(11) (a) Asali, K. J.; Basson, S. S.; Tucker, J. S.; Hester, B. C.; Cortes, J. E.; Awad, H. H.; Dobson, G. R. *J. Am. Chem. Soc.* **1987**, *109*, 5386. (b) Wermer, P. H.; Dobson, G. R. *J. Coord. Chem.* **1989**, *20*, 125.
(12) Zhang, S.; Dobson, G. R. *Polyhedron* **1990**, *9*, 2511.
(13) Dobson, G. R.; Dobson, C. B.; Mansour, S. E. *Inorg. Chem.* **1985**, *24*, 2179.
(14) Zhang, S.; Dobson, G. R. *Inorg. Chem.* **1989**, *28*, 324.
(15) At high [hex]/[CB] much of the (hex)(Ph$_2$MeP)W(CO)$_4$ product is produced directly, without the intermediacy of the (CB)(Ph$_2$MeP)W(CO)$_4$ solvate; thus the signal-to-noise ratio for the disappearance of the solvate is significantly poorer. This was compensated for by averaging more data sets to obtain k_{obsd}.

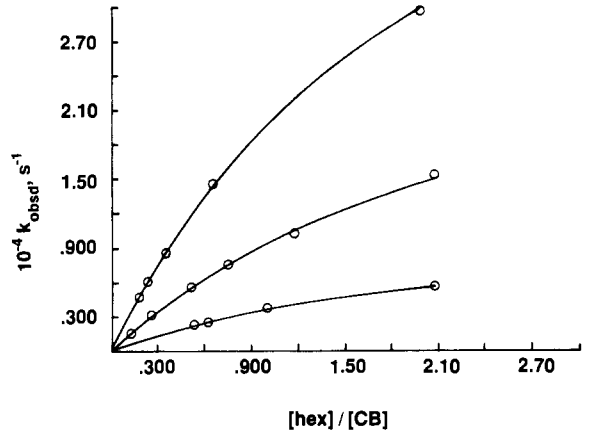

Figure 3. Plots (bottom to top) of k_{obsd} vs [hex]/[CB] for reactions of *cis*-(CB)(Ph_2MeP)W(CO)$_4$ in CB–hex solutions at 5.5, 15.2, and 25.0 °C.

Table I. Rate Constants for Reactions of *cis*-(CB)(η^1-P-ol)W(CO)$_4$ and *cis*-(CB)(Ph_2MeP)W(CO)$_4$ Intermediates in CB–Piperidine Solutions (CB = Chlorobenzene) at Various Temperatures

P-ol	T, °C	$10^{-4}k_a$, s^{-1}	$10^{-4}k_b$, s^{-1}
prdpp	16.1	0.98 (1)	3.5 (2)
	26.1	2.25 (3)	7.7 (4)
	31.1	3.22 (2)	
	37.6	5.16 (6)	15.3 (11)
bdpp	14.5	0.365 (12)	3.8 (3)
	21.1	0.595 (15)	5.6 (2)
	26.1	0.863 (9)	9.16 (17)
	37.6	1.93 (2)	17.4 (4)
pdpp	14.5	0.103 (17)	4.7 (3)
	26.0	0.25 (5)	11.8 (7)
	26.2	0.26 (2)	11.6 (4)
	38.7	0.70 (3)	24.3 (8)
hdpp	14.5	0.161 (12)	4.3 (3)
	21.1	0.294 (13)	6.55 (18)
	26.1	0.44 (2)	9.1 (3)
	37.6	0.98 (4)	20.9 (7)
Ph_2MeP	26.1	(0.06 (2))	6.83 (7)

of a change from second-order kinetics to first-order kinetics with increasing [hex]/[CB]

$$k_{obsd} = k_c[hex]/([CB] + k_d[hex]) \quad (2)$$

consistent with a mechanism consisting of two or more reaction steps, one involving competition for an intermediate by CB and pip. Rearrangement of eq 2 affords

$$1/k_{obsd} = [CB]/k_c[hex] + k_d/k_c \quad (3)$$

Thus, "double reciprocal" plots of $1/k_{obsd}$ vs [CB]/[hex] are expected to be linear, with finite intercepts. Figure 4 indicates that this indeed is the case.

(c) Reaction of Photogenerated *cis*-(CB)(η^1-ol-P)W(CO)$_4$ Transients in CB–*n*-Heptane Mixtures. The influence of [CB] on the rates of chelate ring closure was also investigated by varying [CB] through use of CB–hep solvent mixtures (hep = *n*-heptane). The displacement of hep from photogenerated metal carbonyl transients is much faster than displacement of CB,[1,16] and thus *cis*-(hep)(η^1-ol-P)W(CO)$_4$ intermediates produced in CB/hep solution will have largely decayed on the time scale of CB displacement from *cis*-(CB)(η^1-ol-P)W(CO)$_4$. Plots of k_{obsd} vs 1/[CB] for these reactions at 25 °C (P-ol = prdpp, bdpp, pdpp, hdpp) are illustrated in Figure 5. The plots are curved downward,

(16) (a) Kelly, J. M.; Long, C.; Bonneau, R. *J. Phys. Chem.* **1983**, *87*, 3344. (b) Zhang, S.; Zang, V.; Bajaj, H. C.; Dobson, G. R.; van Eldik, R. *J. Organomet. Chem.* **1990**, *397*, 279.

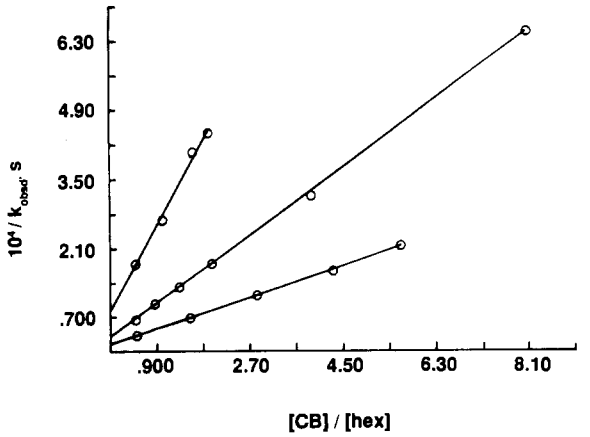

Figure 4. Plots (top to bottom) of $1/k_{obsd}$ vs [CB]/[hex] for reactions of *cis*-(CB)(Ph_2MeP)W(CO)$_4$ in CB–hex solutions at 5.5, 15.2, and 25.0 °C.

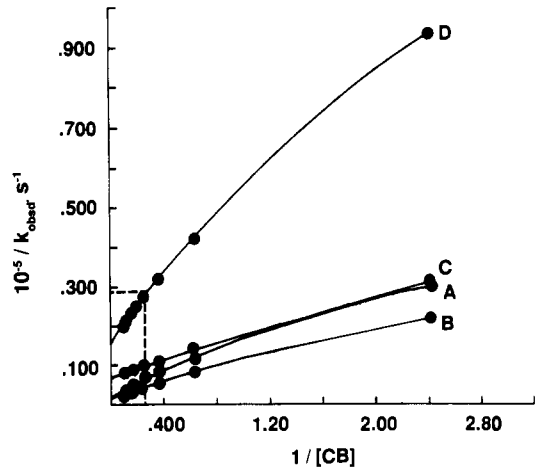

Figure 5. Plots of k_{obsd} vs 1/[CB] for reactions of *cis*-(CB)(η^1-P-ol)W(CO)$_4$ intermediates in CB–hex solutions at 25.0 °C, for P-ol = hdpp (A), pdpp (B), bdpp (C), and prdpp (D).

Scheme IV

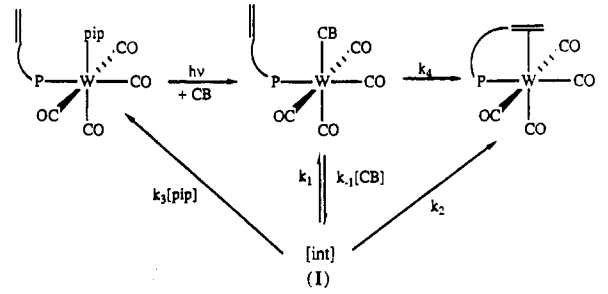

with positive intercepts, indicating a complex mechanism in which increasing concentrations of CB decrease the rates of chelate ring closure.

Discussion

Mechanism. The rate behavior outlined above can be rationalized in terms of the mechanism shown in Scheme IV. The two-term rate laws observed in CB–pip solutions (eq 1, Figure 2) support a mechanism involving competitive reaction pathways for the *cis*-(CB)(η^1-ol-P)W(CO)$_4$ complexes. The intercepts are ascribable to unimolecular chelate ring closure with expulsion of CB, an attribution supported by the zero intercept observed for the kinetics of reactions of *cis*-(CB)(Ph_2MeP)W(CO)$_4$ in CB–pip, where ring closure cannot take place. The slopes are attributable to displacement of CB by pip. Rate behavior of the type shown in eq 1 has been observed and has been similarly

Table II. Rate Constants for Reaction of *cis*-(CB)(Ph_2MeP)$W(CO)_4$ with 1-Hexene in Chlorobenzene at Various Temperatures

T, °C	$10^4k_1k_2/k_{-1}$, s^{-1}	10^4k_1, s^{-1}	k_2/k_{-1}
5.5	0.51 (2)	1.2 (2)	0.43 (8)
15.2	1.36 (1)	3.4 (2)	0.40 (4)
25.0	2.81 (4)	6.8 (7)	0.41 (4)

attributed in pulsed laser flash photolysis studies of (η^2-NP)M-$(CO)_4$ complexes (NP = bidentate ligand containing phosphine and amine functional groups; M = Cr, Mo, W).[13,17]

When a steady-state concentration of the intermediate (I) is presumed, the rate law consistent with Scheme IV and expressed in terms of the pseudo-first-order rate constants, k_{obsd}, is

$$k_{obsd} = \{k_1k_2/(k_{-1}[CB] + k_2 + k_3[L]) + k_4\} + k_1k_3[L]/(k_{-1}[CB] + k_2 + k_3[L]) \quad (4)$$

For studies where the rate law in eq 1 is observed, L = pip and [pip]/[CB] < 0.13. It thus is reasonable to expect that $k_{-1}[CB] \gg k_3[L]$ and that [CB] is essentially constant over this [pip]/[CB] concentration range. It also will be demonstrated (vide infra) that under the conditions of this study $k_{-1}[CB] \gg k_2$. Thus, eq 4 simplifies to

$$k_{obsd} = (k_1k_2/k_{-1}[CB] + k_4) + k_1k_3[L]/k_{-1}[CB] \quad (5)$$

of the same form as the rate law given in eq 1. The rate constants k_a ($=k_1k_2/k_{-1}[CB] + k_4$) and k_b ($=k_1k_3/k_{-1}$; eq 1 and 5), are presented in Table I.

The term governed by k_b, eqs 1 and 5, was further studied through investigation of the reaction of photogenerated *cis*-(CB)-(Ph_2MeP)$W(CO)_4$ with 1-hexene (hex, = L; Scheme III) for the concentration range 0.12 < [hex]/[L] < 2.1, over which non-limiting rate behavior was observed. For the mechanism given in Scheme IV

$$k_{obsd} = k_1k_2'[hex]/(k_{-1}[CB] + k_2'[hex]) \quad (6)$$

where k_2' is now a bimolecular rate constant, for reaction of hex with the *cis*-(CB)(Ph_2MeP)$W(CO)_4$ intermediate. For this rate law, plots of k_{obsd} vs [L]/[CB] are expected to be concave downward, as observed in Figure 3. Rearrangement of eq 6 affords

$$1/k_{obsd} = 1/k_1 + k_{-1}[CB]/k_1k_2'[hex] \quad (7)$$

Thus, plots of $1/k_{obsd}$ vs [CB]/[hex] are expected to be linear, with intercepts $1/k_1$ and slopes k_1/k_1k_2'. Values for the rate constants k_1k_2'/k_{-1}, k_1, and k_2'/k_{-1}, derived from the slopes and intercepts, are presented in Table II. In view of the linearity of these plots, it may be concluded that displacement of CB by hex takes place exclusively via a mechanism involving initial loss of CB.

Further insight into the "ring-closure" pathways represented by the intercepts, k_a

$$k_a = k_1k_2/(k_{-1}[CB] + k_2 + k_3[L]) + k_4 \quad (8)$$

in the four *cis*-(CB)(η^1-ol-P)$W(CO)_4$ intermediates generated after flash photolysis (eqs 1 and 4) was obtained by varying the CB concentration in the absence of a nucleophile, L. In the absence of a trapping nucleophile, L, eq 8 simplifies to

$$k_a = k_1k_2/(k_{-1}[CB] + k_2) + k_4 = k_{obsd} \quad (9)$$

Note that under the conditions of this study [CB] varies widely so it is not always the case, as it was for eq 4, that $k_{-1}[CB] \gg k_2$. Plots of k_{obsd} vs 1/[CB], illustrated in Figure 5, are concave downward and, with one exception, have positive intercepts. Thus,

(17) Mansour, S. E.; van Zyl, G. J.; Dobson, G. R. Manuscript in preparation.

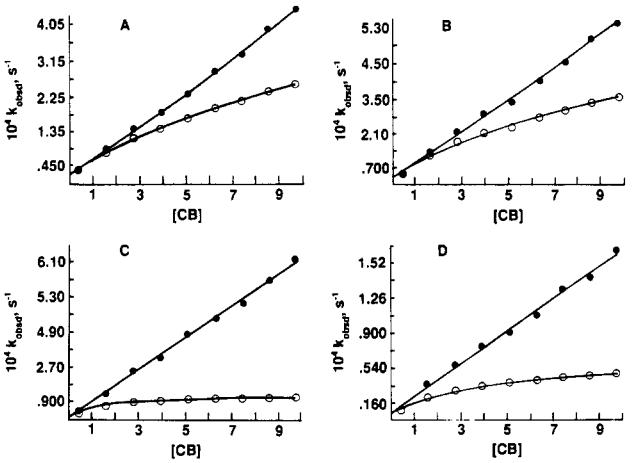

Figure 6. Plots of $1/k_{obsd}$ vs [CB] (curved) and $1/(k_{obsd} - k_4)$ vs [CB] (linear) for chelate ring closure in *cis*-(CB)(η^1-P-ol)$W(CO)_4$ intermediates in CB–hep solutions at 25.0 °C, for P-ol = hdpp (A), pdpp (B), bdpp (C), and prdpp (D).

Table III. Rate Constants for Chelate Ring Closure in *cis*-(CB)(η^1-P-ol)$W(CO)_4$ Intermediates in Chlorobenzene–*n*-Heptane Solutions at Various Temperatures

P-ol	T, °C	$10^{-4}k_1$, s^{-1}	$10^{-4}k_1k_2/k_{-1}$, s^{-1}	$10^{-3}k_4$, s^{-1}
prdpp	5.5		0.98 (6)	3.26 (8)
	15.3		3.0 (2)	7.1 (3)
	25.0		5.4 (3)	14.8 (4)
		13 (3)[a]	5.9 (1)[a]	14.5 (6)[a]
bdpp	5.5		0.21 (3)	1.57 (4)
	14.5		0.56 (3)	2.92 (4)
	25.0		1.11 (5)	6.82 (7)
		2.6 (3)[b]	1.18 (2)[a]	6.7 (1)[a]
pdpp	5.5		0.266 (1)	0.204 (2)
	14.5		0.535 (7)	0.52 (1)
	25.0		1.47 (7)	1.16 (3)
		3.2 (6)[a]	1.54 (2)[a]	1.2 (1)[a]
hdpp	5.5		0.39 (3)	0.28 (4)
	14.5		0.78 (2)	0.83 (3)
	25.0		2.03 (6)	1.72 (9)
		4.6 (6)[a]	2.29 (2)[a]	1.6 (1)[a]

[a] Value calculated from the best linear fit of the plot of $1/(k_{obsd} - k_4)$ vs [CB]. [b] Calculated from k_1k_2/k_{-1} assuming k_2/k_{-1} = 0.46 (4); see text.

they are qualitatively consistent with the nonlinear plots expected on the basis of eq 9. The expression for k_{obsd} in terms of the rate constants defined in Scheme IV (eqs 1, 4, and 9) can be rearranged to

$$1/(k_{obsd} - k_4) = k_{-1}[CB]/k_1k_2 + 1/k_1 \quad (10)$$

For this rate law, plots of $1/(k_{obsd} - k_4)$ vs [CB] are thus expected to be linear, with intercept $1/k_1$ and slopes k_{-1}/k_1k_2. An iterative computer program was employed to determine the value of k_4 which afforded the best linear fit of these plots. Figure 6 illustrates plots of $1/k_{obsd}$ vs [CB] and $1/(k_{obsd} - k_4)$ vs [CB] at 25 °C for chelate ring closure in each of the four *cis*-(CB)(η^1-Pol)$W(CO)_4$ intermediates. The excellent linear fit of the latter data lends support to a mechanism involving two competitive desolvation pathways and permits evaluation of the rate constants k_1, k_4, and k_2/k_{-1} for the transients containing prdpp, pdpp, and hdpp. However, for P-ol = bdpp, the intercept of the plot of $1/(k - k_4)$ vs [CB] (eq 10) does not afford statistically meaningful values of k_1 (and, therefore, of k_2/k_{-1}). Values of the rate constants from data at three temperatures are presented in Table III. Values of k_2/k_{-1} calculated from data presented in this table for prdpp, pdpp, and hdpp and given in Table II for Ph_2MeP are 0.46 (13), 0.47 (10), 0.50 (7), and 0.41 (5), respectively, and thus are the same, within experimental error. It is not unreasonable to presume that k_2/k_{-1} for bdpp also is similar (the average value of k_2/k_{-1}

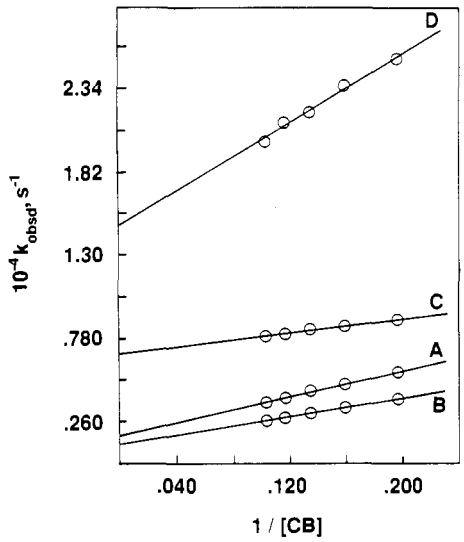

Figure 7. Plots of k_{obsd} vs 1/[CB] at [CB] ≥ 5 M for chelate ring closure in *cis*-(CB)(η^1-P-ol)W(CO)$_4$ intermediates in CB–hep solutions at 25.0 °C, for P-ol = hdpp (A), pdpp (B), bdpp (C), and prdpp (D).

Table IV. Contributions of Dissociative and Interchange Reaction Paths to Rates of Desolvation via Chelate Ring Closure

P-ol	$10^{-3}k_{calcd}$,[a] s^{-1}	$10^{-3}k_{exptl}$,[b] s^{-1}	% dissociative[c]
prdpp	20.3 (7)	22.5 (3)	27 (2)
bdpp	7.95 (12)	8.63 (9)	14 (1)
pdpp	2.66 (10)	2.49 (47)	56 (4)
hdpp	3.79 (15)	4.36 (21)	55 (4)

[a] Calculated from values of k_1, k_1k_2/k_{-1}[CB], and k_4 according to eq 10 from data at 25.0 °C. [b] Experimentally determined as k_a (eq 2) from data at 26.0–26.1 °C. [c] Determined as percentages from k_1k_2/k_{-1}[CB] and k_4 at 25.0 °C.

for Ph_2MeP, prdpp, pdpp, and hdpp is 0.46 (4)). Using this value for k_2/k_{-1} for bdpp, one can calculate the corresponding value for k_1 which is given in Table III.

Since values of k_2/k_{-1} are 0.46 (4), where [CB] is high (>5 M), k_{-1}[CB] ≫ k_2, and eq 4 becomes

$$k_{obsd} = k_4 + k_1k_2/k_{-1}[CB] \qquad (11)$$

Thus, where [CB] is >5 M, plots of k_{obsd} vs 1/[CB] are expected to be linear, with intercepts k_4 and slopes k_1k_2/k_{-1}. These plots (the data are enclosed in the box in Figure 5) are illustrated in Figure 7. The values of k_4 and k_1k_2/k_{-1} obtained from these plots, also given in Table III, are in good agreement with those obtained through a fit of plots of $1/(k_{obsd} - k_4)$ vs [CB]. This exercise also confirms, as was assumed above (eq 5) that $k_2 \ll k_{-1}$[CB] in dilute CB/pip solutions.

The values of k_1, rate constants for unimolecular dissociation of CB from the *cis*-(CB)(η^1-P-ol)W(CO)$_4$ intermediates, which vary pdrpp (13 (3)) > hdpp (4.6 (6)) ≈ pdpp (3.2 (6)) ≈ bdpp (2.6 (3)); all values × 10^{-4} s^{-1}), are largely dependent upon the steric bulk (cone angle)[18] of P-ol.[6]

The rate constants k_1, k_1k_2/k_{-1}, and k_4 obtained from data for CB–hep solutions (Table III) comprise the rate constants k_a (eq 1), as is shown in eq 9. It thus is possible to analyze k_a, obtained directly as intercepts of the plots of $1/k_{obsd}$ vs [CB]/[pip], in terms of the relative contributions of the two ring-closure pathways to desolvation (dissociative and interchange; Scheme IV). This analysis is given in Table IV. Values for the rate constants comprising k_a afford values of k_a which are in good agreement with those determined experimentally from the kinetic studies for reactions of the four complexes (L = prdpp, bdpp, pdpp, hdpp) in pip–CB solutions (Table I). The consistency of the data demonstrates that rate behavior is the same, within experimental error, in both CB and in CB–hep solutions and strongly supports the proposed mechanism (Scheme IV).

Nature of the Reaction Intermediate. A question arises as to the nature of the intermediate(s) (I, Scheme IV) which exist along the reaction coordinate leading from CB dissociation to ring closure. Evidence to be presented in the discussion of activation parameters (vide infra) indicates that it is not a coordinatively-unsaturated species such as II since the activation enthalpy observed for CB dissociation from *cis*-(CB)(η^1-ol-P)W-(CO)$_4$ would appear to be anomalously low, suggesting stabilization of I through some bonding interaction. Two possible intermediates, III and IV, envision agostic interactions between W and hydrogens in P-ol. The possible intermediacy of such species is supported by the "competition ratios", k_2/k_{-1}, of the rates of chelate ring closure to bimolecular interaction of the solvent with intermediate I (Scheme IV). As noted above, where the data have permitted their direct evaluation, for prdpp, pdpp, and hdpp, these competition ratios are the same, within experimental error, 0.46 (13), 0.47 (10), and 0.50 (7). Moreover, the competition ratio for reaction of the intermediate where L = Ph_2MeP with hex is 0.41 (5), also within one standard deviation of those for the three complexes containing chelate rings. If one assumes, for the moment, that values of k_{-1}, the rate constants for reaction of CB with I (Scheme IV) are similar, the competition ratios represent relative values of k_2. From them, values for the "effective molarities" of the free end of the chelate ring, k_{intra}/k_{inter}, as the ratios of k_2 for chelate ring closure (L = prdpp, pdpp, and hdpp) and k_2' for bimolecular reaction of I (Scheme IV) with hex; L = Ph_2MeP) can be calculated. These values, 1.1 (5), 1.1 (3), and 1.2 (4) M, respectively, contrast sharply with others which have been reported, e.g., for lactone formation, which vary over several orders of magnitude for the range of chelate ring sizes in question.[7] The values also are inconsistent with the observation that solvent displacement takes place via an interchange pathway upon chelate ring closure, but exclusively via solvent dissociation for the monodentate ligand, hex. These observations indicate that chelate ring size, or for that matter, the presence or absence of a bidentate ligand, has no influence on rates of reaction of I (Scheme IV). Based on the observed effective molarities, it is most reasonable to assume that the ground states and transition states for all four of these complexes are very similar in nature and that chelate ring closure via formation of W–olefin linkages is not involved in the rate-determining steps governed by k_2, i.e., *that chelate ring closure takes place after the rate-determining steps.* Thus these data support the possible intermediacy of III, illustrated for P-ol = bdpp in Scheme V, but also applicable to other P-ol ligands and to Ph_2MeP. The mechanism involving such as intermediate would envision CB displacement from the solvated species produced after flash photolysis via chelate ring closure through formation of a C–H–W agostic bond.[19] Such intermediates, which involve interactions of ortho hydrogens in arylphosphine ligands with transition metals, have been well-documented.[19] If this type of agostic interaction is present along the reaction coordinate to solvent displacement, existence of a coordinatively-unsaturated reaction intermediate need not be invoked for this process.[20] The intermediate shown in IV would appear less probable to react via rate constants k_{-1}

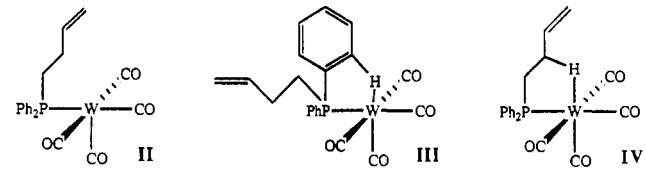

(18) Tolman, C. A. *Chem. Rev.* **1977**, *77*, 313.

(19) (a) Brookhart, M.; Green, M. L. H. *J. Organomet. Chem.* **1983**, *250*, 395. (b) Brookhart, M.; Green, M. L. H.; Wong, L.-L. *Prog. Inorg. Chem.* **1988**, *36*, 2.

(20) Lee, M.; Harris, C. B. *J. Am. Chem. Soc.* **1989**, *111*, 8963.

Scheme V

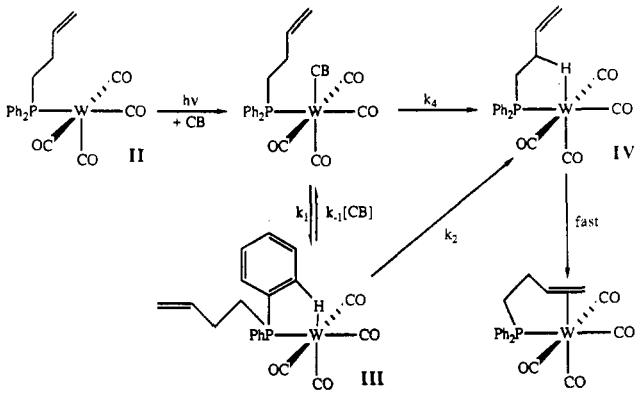

Table V. Activation Parameters for the Reactions

	prdpp	bdpp	pdpp	hdpp	Ph_2MeP	set
			Enthalpy (kcal/mol)			
ΔH^*_1					12.1 (8)	1
ΔH^*_4	11.2 (6)	11.9 (6)	14.1 (7)	12.7 (11)		2
ΔH^*_{12-1}	14.4 (3)	13.4 (13)	15.3 (2)	13.4 (4)	13.6 (3)	3
ΔH^*_{13-1}	11.7 (6)	11.4 (7)	11.6 (6)	11.6 (4)		4
ΔH^*_{4+12-1}	13.1 (2)	12.24 (7)	13.6 (4)	13.1 (4)		5
			Entropy [cal/(K mol)]			
ΔS^*_1					3.8 (26)	1
ΔS^*_4	−2.1 (22)	−1.2 (20)	+2.9 (23)	−1.4 (40)		2
ΔS^*_{12-1}	11.4 (12)	5.2 (46)	11.8 (8)	6.0 (12)	7.3 (20)	3
ΔS^*_{13-1}	3.1 (19)	2.3 (23)	3.4 (20)	3.3 (12)		4
ΔS^*_{4+12-1}	5.7 (5)	0.71 (22)	2.8 (13)	2.3 (12)		5

and k_2 since such a pathway would not be accessible for Ph_2MeP, and yet the competition ratio, k_2/k_{-1}, for this ligand is similar to those observed for the P-ol ligands. However, the observation that the pathway governed by k_4 is accessible for the P-ol ligands but not for Ph_2MeP leads one to speculate that intermediates such as IV stabilize the transition states along this competitive ring-closure pathway; evidence has been presented which suggests that rearrangement of species such as IV to afford the thermodynamically-stable ring-closure products may be very rapid.[21] This would account for the lack of reversibility of the reaction step governed by k_4.

Activation Data. Activation data for all systems studied are presented in Table V. The values of the enthalpies and entropies of activation vary over relatively narrow ranges, and within a series of five solvates (for the four P-ol ligands and for Ph_2MeP) there are no discernable trends for a given rate constant. However, since trends among rate constants are noted among series of solvates, the series are listed as "sets" (1–5) within Table V. Several informative comparisons may be noted. Solvent displacement from the four *cis*-(CB)(η^1-P-ol)$W(CO)_4$ intermediates governed by k_4 (set 2) takes place with slightly lower average enthalpies of activation, 12.7 (7) kcal/mol, and more negative entropies of activation, +0.6 (19) cal/(K mol), than does the competitive pathway governed by k_1k_2/k_{-1} (set 3), 13.9 (5) kcal/mol and 8.1 (22) cal/(K mol), respectively. The difference, which is barely significant statistically, suggests similar stabilization in the transition states leading to chelate ring closure, as would be the case were the intermediates produced along these reaction pathways each to exhibit agostic W–H bonding. The entropies of activation for the path governed by k_1, k_{-1}, and k_2, while positive, are less positive than one might expect for a purely dissociative process. Comparisons of sets 2 and 3 with set 5 reveal, as would be anticipated, that activation parameters derived separately from these pathways (sets 2 and 3; vide supra) bracket those derived for these processes where they are competitive (set 5, from k_a, Table I, eqs 1 and 4), $\Delta H^* = 13.0$ (4) kcal/mol, $\Delta S^* = 2.8$ (14) cal/(K mol). The enthalpies and entropies of activation for chelate ring closure via the pathway governed by k_1, k_2, and k_{-1}, with average values of 14.0 (5) kcal/mol and +8.4 (22) cal/(K mol), respectively, are also very similar to those observed for the dissociative pathway for CB replacement by hex from *cis*-(CB)-$(Ph_2MeP)W(CO)_4$, 13.9 (7) kcal/mol and +8.9 (25) cal/(K mol), respectively. Subtraction of the corresponding activation parameters for CB dissociation from *cis*-(CB)$(Ph_2MeP)W(CO)_4$ ($\Delta H_1^* = 14.1$ (10) kcal/mol, $\Delta S_1^* = 11.5$ (35) cal/(K mol), set 1) from those determined from k_1k_2/k_{-1} (set 3, $\Delta H^* = 14.0$ (5), $\Delta S^* = 8.4$ (22) cal/(K mol), vide supra) afford the activation parameters $\Delta H_2^* - \Delta H_1^* = +0.2$ (17) kcal/mol and $\Delta S_2^* = 0.5$ (47) cal/(K mol) for the "competition ratios", k_2/k_{-1}, zero, within experimental error. These values provide additional support for the view that this reaction pathway is similar for complexes containing Ph_2MeP and P-ol and involves chelate ring closure only after the reaction's rate-determining steps.

However, comparison of data sets 3 and 4, of activation parameters derived from k_2 and k_3, rate constants for reactions of intermediate I (Scheme IV) with olefin functionalities or with pip, affords average differences for the enthalpies and entropies of activation, 2.4 (6) kcal/mol and 5.4 (26) cal/(K mol). This difference suggests that the stronger nucleophile, pip, displaces the (presumed) agostic interaction in I (Scheme IV) via a pathway which involves some bond-making in the transition state and that this intermediate is able to discriminate significantly among incoming nucleophiles. This would not be the case were the intermediate to contain a center of coordinative unsaturation, for which rates of solvation have been observed to be extremely rapid[22] and, consequently, for which activation enthalpies (and discriminating abilities) are expected to be quite small.

In view of current interest in the strengths of interaction of various solvent molecules with coordinatively-unsaturated metal carbonyl transients, evidence supporting significant M–H–C agostic bonding in transition states leading to desolvation is of particular interest. Two methods, the first involving the use of time-resolved pulsed laser photoacoustic calorimetry (TR-PAC)[23,24] and the second based upon the evaluation of activation enthalpies for unimolecular metal–solvent bond fission,[3,25] have been employed for the estimation of solvent–metal bond strengths in solvated intermediates of the group 6 metals. The second method depends critically on the assumption that the transition state leading to desolvation is similar in energy to the presumed coordinatively-unsaturated intermediate produced via M–solvent bond dissociation; bond strengths determined through use of TR-PAC depend upon other assumptions. Unfortunately, few direct comparisons between bond strengths determined through use of the two methods are available. However, the enthalpies of activation for CB displacement reported here would not appear to represent the W–CB bond strengths, which, as photoacoustic calorimetry data indicate, should be significantly greater. Metal–*n*-heptane bond strengths (metal = Cr, W) have been determined by Burkey and co-workers to be 9.6 (23) and 13.4 (20) kcal/mol,[24] suggesting that W–solvent bonds are significantly stronger, perhaps by ca. 4 kcal/mol, than are Cr–solvent bonds. The Cr–CB bond strength has been determined through similar procedures to be 18.1 (47) kcal/mol,[26] indicative of a W–CB bond strength of ca. 22 kcal/mol. This estimate can be compared to activation enthalpies determined through this investigation (Table V), all of which are within the range 11–15 kcal/mol. The difference between the CB–W bond strength estimated on the basis of TR-

(21) Xie, X.; Simon, J. D. *J. Am. Chem. Soc.* **1990**, *112*, 1136.

(22) Langford, C. H.; Moralejo, C.; Sharma, D. K. *Inorg. Chim. Acta* **1987**, *126*, L11.

(23) Yang, G. K.; Vaida, V.; Peters, K. S. *Polyhedron* **1988**, *7*, 1619.

(24) Morse, J.; Parker, G.; Burkey, T. J. *Organometallics* **1989**, *7*, 2471.

(25) Zhang, S.; Dobson, G. R. *Inorg. Chim. Acta* **1991**, *181*, 103.

(26) (a) Burkey, T. J. *Abstracts of Papers* 199th National Meeting of the American Chemical Society, Boston, 1990; American Chemical Society: Washington, DC, 1990. (b) Burkey, T. J. Personal communication, 1990.

PAC data and, for example, the enthalpy of activation for displacement of CB from *cis*-(CB)(Ph_2MeP)$W(CO)_4$ by hex, 12.1 (8) kcal/mol, supports stabilization of the transition state through agostic hydrogen bonding in the systems studied here, consistent with the mechanistic picture for solvent displacement which has been presented.

Acknowledgment. The support of this research by the National Science Foundation (Grant CHE-880127) and the Robert A. Welch Foundation (Grant B-0434) is gratefully acknowledged. Some experiments and data analysis were carried out at the Center for Fast Kinetics Research (CFKR), University of Texas at Austin. The CFKR is supported jointly by the Biotechnology Program of the Division of Research Resources of the National Institutes of Health (RR00886) and by the University of Texas at Austin.

Supplementary Material Available: Tables of ^1H and ^{13}C NMR data for *cis*-(pip)(Ph_2MeP)$W(CO)_4$, values of k_{obsd} for reactions of *cis*-(CB)(Ph_2MeP)$W(CO)_4$ and *cis*-(CB)(η^1-P-ol)$W(CO)_4$ intermediates in CB/pip solutions at various temperatures, values of k_{obsd} for reactions of *cis*-(CB)(Ph_2MeP)$W(CO)_4$ with 1-hexene in chlorobenzene solution at various temperatures, and values of k_{obsd} for chelate ring closure in *cis*-(CB)(η^1-P-ol)$W(CO)_4$ intermediates in CB/*n*-heptane solutions at various temperatures (13 pages). Ordering information is given on any current masthead page.